

10 Powder flow and storage

Pumping fluids is simple: you need a pump and some pipework. The higher the viscosity, the higher the pressure drop and, therefore, pump and energy costs. Much is known about how to characterise and specify a fluid system. What is the equivalent for dry particles? Also, tanks can be used to store liquids, but how should we store powders to ensure that they can be reliably used within our process? This is a subject that has received considerable attention over many centuries and is still a long way from a complete understanding. This chapter considers simple characterisation based on solid properties and a one-dimensional particle mechanics analysis. A more thorough description is possible by Discrete Element Analysis, see Chapter 7.

It would be a mistake to assume that the problem is just one of ensuring that the powder flows in a hopper, or down a chute. There are many recorded instances of process difficulties due to powders suddenly flowing too easily! If a hopper is discharging into a process and suddenly the powder surges out, it is likely that it will overflow the process vessels and cause disruption: this is called a *powder flood*. An example of a powder flood in nature is an avalanche and it is, of course, potentially very dangerous. Process operators can be killed in a powder flood, so these must be avoided at all costs. Powder flow in a controlled and predictable fashion is desired. Floods are usually associated with *aerated powders*, in which gas is mixed with the powder and it behaves in a fluidised fashion, see Chapter 7.

10.1 Powder properties

An understanding of particle behaviour starts with a consideration of particle properties and some basic techniques to measure them. One of the simplest measurements is the *angle of repose*, which is illustrated in Figure 10.1, and is often assumed to be the angle that the hopper needs to exceed in order to assure powder flow. This may be acceptable for *free flowing* powders, and the angle is typically 30°, but in most cases this ignores the tendency for particles to form a cohesive structure depending upon how they have been treated. Pouring the powder into an upside down funnel and then carefully removing the funnel to leave the heap in place can be used to measure the angle. Alternative techniques include measuring the angle of slide and the angle of rotation, as illustrated in Figure 10.2.

The particle size distribution has a complex effect on the angle of repose and a graph of the angle plotted, against the percentage of fines present, usually shows a minimum, see Figure 10.3. The angle of repose is a property of a powder that does not exist in a liquid and it is not a very consistent measurement for a powder because most powders exhibit some degree of cohesiveness.

To flow or stick?		
Property	Free flowing	Difficult flowing
Size	>400 μm	<100 μm
Range	narrow	wide
Shape	spheres	needles
Moisture	not too low*	high & none
Internal friction	low	high

* a certain amount of moisture may help to lubricate the flow and to prevent any electrostatic attraction between particles from stopping the flow.

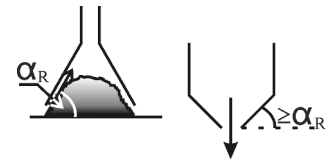


Fig. 10.1 Angle of repose and its possible relevance to hopper design

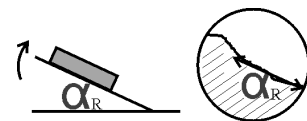


Fig. 10.2 Alternative measures

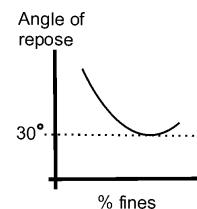


Fig. 10.3 Influence of fines on angle of repose

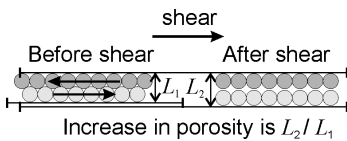


Fig 10.4 Two planes needing to dilate (open out) before moving

Porosity is *isotropic*: i.e. the same in all directions, but the assumption here is that the overall porosity increase is due to expansion in one plane (i.e. height).

The *bulk density* is the combined density of the powder and the void space (i.e. porosity see Figure 3.1). Hence the bulk density is the same as the mean suspension density, equation (6.12), but as the fluid is air its contribution to the mean density is ignored. Thus

$$\rho_b = (1 - \varepsilon)\rho_s \tag{10.1}$$

However, the bulk density is a function of porosity, i.e. how the powder has been treated. To standardise this the *tap density* is used (BS 3483). The powder (and voids) volume is measured in a measuring cylinder type vessel after 0 to 800 taps and the powder weighed. This provides a more consistent density than the bulk.

Another property that powders possess, but liquids do not, is that of *dilatancy*. This arises from particles resting on each other such that a shear plane of particles must rise vertically before it is possible for the plane to move horizontally, as illustrated in Figure 10.4. As the planes move apart from each other the porosity increases. The porosity at which the powder can shear is known as the *critical porosity*. Dilatancy is important for powders flowing in chutes; in Figure 10.5 a box is provided at the point where the powder changes direction, to allow for the powder to dilate, or expand. Without the expansion box the powder may be prevented from dilating and, therefore, cease to flow.

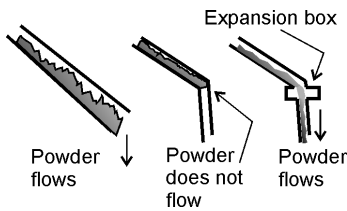


Fig. 10.5 Expansion box in flow chute

Powders have the ability to sustain shear forces better than fluids. Thus, it is possible to walk on a bed of powder, such as a sandy beach. The weight of an object on the powder is transmitted through a network of contacts within the powder compact to the underlying base, or to the walls of a container. Hence, Archimedes' buoyancy principle does not occur: the 'up-thrust' experienced by a body submerged, or partially submerged, is *not* equal to the weight of the material displaced. The up-thrust may be equal to the entire weight of the body - just like a solid surface. Unlike fluids, there isn't a linear increase in pressure with depth of particles. In fact, the pressure stabilises after a short distance and the rate of discharge from a hopper will, therefore, be substantially constant. The rate of discharge (M_p) for free flowing powders has been correlated using the following empirical equation

$$M_p = \frac{\pi}{4} \rho_b \sqrt{gB^5 2 \tan \theta_H} \tag{10.2}$$

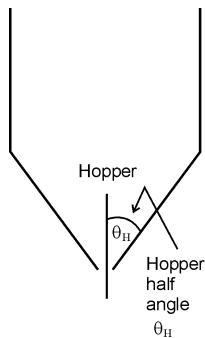


Fig. 10.6 Hopper half angle

where B is the opening diameter and θ_H is the hopper half angle; i.e. the angle from the vertical, see Figure 10.6. Note that this equation does not include powder height. However, powders may form a *stable arch* over the opening and block the powder flow, see later.

Whenever powders flow there is an opportunity for the powder to *segregate* by, primarily, size and density difference (and other secondary factors such as rotational inertia). This will occur in heaps, hoppers, mixers, conveyors, etc. By contrast, miscible fluids do not *un-mix* like this.

10.2 Flow patterns and stress in a hopper and silo

A *hopper* is the conical, or converging, section of a powder storage vessel; the *bin* is the parallel sided section, usually cylindrical or rectangular, and the word *silo* is used to cover the entire vessel. However, these terms are often used interchangeably. There are two main flow types that describe how powder discharges from a silo and these are illustrated in Figure 10.7. In *mass flow* the flow pattern is often described as: first in, first out and in *core*, or *funnel*, flow the pattern is last in, first out. In true mass flow the powder at the edges of the hopper has to accelerate and shear over that towards the centre: as it has a longer distance to travel to the discharge hole. Dilatancy is required at this point and the stress on the hopper is greatest here.

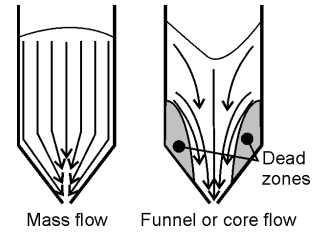


Fig. 10.7 Flow patterns during hopper discharge

A hopper may acceptably operate under funnel or core flow conditions so long as *piping*, or *rat holing* doesn't occur. These two terms refer to a silo in which the storage capacity consists substantially of stationary powder with just a hole within the silo taking newly deposited material from the top straight to the bottom and discharge. Hence, there is no net storage capacity within the silo. Table 10.1 compares the advantages and disadvantages of the two types of flow.

Table 10.1 Flow patterns in a silo - italicised text indicates preferred behaviour

Powder stresses inside a hopper may be analysed by Janssen's method of differential slices. Consider a slice dz at a height z , the downward force (vertical pressure times applied area) is

$$\frac{\pi D^2}{4} P_v$$

The resultant solids stress (i.e. equivalent to pressure in a fluid and equal to force over area) is

$$\frac{\pi D^2}{4} \delta P_v$$

Another force comes from the wall. If the horizontal stress at the wall is P_h and the coefficient of friction is μ_w , then the wall support force is $\mu_w (P_h \pi D \delta z)$ (10.4)

The weight (i.e. force) of solids in the differential slice is $\frac{\pi D^2}{4} \delta z \rho_b g$ (10.5)

Combining the forces: upthrust + wall friction = weight

$$\frac{\pi D^2}{4} \delta P_v + \mu_w P_h \pi D \delta z = \frac{\pi D^2}{4} \delta z \rho_b g$$

giving

$$\frac{dP_v}{dz} + \frac{4\mu_w P_h}{D} = \rho_b g$$
 (10.6)

The problem is in relating the horizontal with the vertical stresses, or pressures. If the material in the hopper is a liquid these two pressures are the same (Pascal's principle). However, consider a stack of coins,

Mass flow	Core flow
Uniform flow and well controlled	Erratic flow can cause powder to flood
No dead regions - no perishable spoilage	Static zones at sides - which may empty at the end
Channelling and bridging absent	Piping may occur
Less segregation	Particles roll during discharge
Tall and thin	Higher capacity for capital cost
High stress at direction changes	Arrangement may relieve wall stresses

Janssen's k_J factor
 $P_h = k_J P_v$
 where $k_J = 0$ for coins,
 where $k_J = 1$ for liquids,
 and
 $0 < k_J < 1$
 for powders.

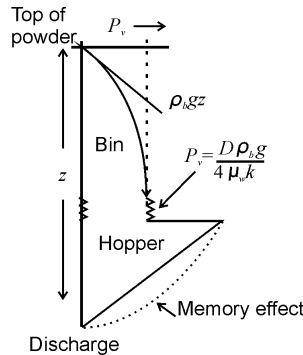


Fig. 10.8 Stresses inside a silo

one on top of another, in air. In this case the horizontal pressure is zero – there is no force accelerating the coins sideways, nor any reaction force needed to prevent this. Now, as powders have properties between that of fluids and continuous solid bodies (such as a stack of pennies), it would be expected that we could write

$$P_h = k_J P_v$$

see box. This was Janssen's assumption. Substituting this simple relation into equation (10.6) and integrating (using integrating factors) results in the following equation

$$P_v = \frac{\rho_b g D}{4\mu_w k_J} [1 - \exp(-4\mu_w k_J z / D)] + P_{v0} \exp(-4\mu_w k_J z / D) \quad (10.7)$$

where P_{v0} is the pressure at $z=0$, called the *surcharge* or uniform stress applied at the top of the powder. For $P_{v0}=0$ and at small values of z

$$P_v = \frac{\rho_b g D}{4\mu_w k_J} \frac{4\mu_w k_J}{D} z \quad \text{as } \exp(-Az) \approx 1 - Az \text{ for low } z \quad (10.8)$$

Thus, $P_v = \rho_b g z$ – a similar result to that of liquids *but* only for small values of z . At large values of z the exponential term disappears, hence

$$P_v = \frac{\rho_b g D}{4\mu_w k_J} \quad (10.9)$$

i.e. pressure asymptotes to the above uniform value. The results from these equations are illustrated in Figure 10.8.

Janssen's work was important because it showed that stress is not transmitted in a similar way to hydraulic head, and *wall friction has a very significant influence on the internal powder stresses*. However, the assumption of a constant coefficient linking the vertical and horizontal stresses has no theoretical justification. Also, arches can be formed, suggesting that the surface of interest is not planar and that the stress in a plane is not uniform. Nevertheless, it provides a useful semi-theoretical analysis of stress inside a hopper. Practical measurements have supported the above analysis: powder stress does build up to a constant value within a parallel sided bin. At the position of the start of the hopper (converging section) the stress rapidly increases, see the section on dilatancy, followed by diminishing values as the hopper diameter then reduces to a value of zero at the outlet. However, measurements show that the powder retains some extra stress over what is expected in the hopper section – this is the *memory effect* included on Figure 10.8.

10.3 Hopper opening and angle

The correct design, or operation, of a hopper to ensure consistent (mass flow) discharge is based upon two factors: providing a steep enough *hopper angle* and ensuring that the discharge *opening* is wide enough. Laboratory tests are performed under conditions of stress and consolidation that are similar to that expected in the hopper.

Values of the required stress to break a *stable arch* are deduced and the hopper is designed to provide these conditions with this powder. This is illustrated in Figure 10.9. Although most of the following text considers hopper design, the principles are more generally applicable to powder flow and characterisation than simply hopper design: i.e. the *Powder Flow Function* (PFF) or sometimes called the *Material Flow Function*, characterises the ease, or otherwise, of powder transport and storage.

During the discharge of a mass flow silo there is a possibility that the powder flow may stop, or become intermittent, due to the formation of a stable arch within the hopper. The reasoning is that the particles interlock to form a stable arch over the opening much like bricks in an arched bridge. In practice, sufficient force should be provided by the system, if correctly designed, to break this bridge if it forms. Firstly, a force balance can be used to determine the magnitude of forces present in this powder bridge. Consider a hopper with an opening of diameter B and a slice of powder of depth Δh . If an arch forms there will be air on one side and powder on the other. The powder within the arch will have a yield stress; given sufficient stress above the arch it will break. This value of stress is called the *unconfined yield stress* (f_c): unconfined because the powder is open to air on one side. An illustrative balance (taking moments from the wall) on the plane forming the arch provides the following result, see Figure 10.9

$$f_c \text{Area}L = W \frac{B}{2} \quad (10.10)$$

where W is the powder weight, B can be taken to be the hopper opening diameter and L is the linear distance that the arch can be said to act over. The force from the weight of powder is

$$W = \text{Area} \Delta h \rho_b g \quad (\text{Newtons}) \quad (10.11)$$

Combining these two equations gives the following result

$$f_c = \rho_b g B \frac{\Delta h}{2L} = \frac{\rho_b g B}{H(\theta)} \quad (10.12)$$

where L , and hence $H(\theta)$, is a function of the geometry of the opening. Thus the minimum hopper opening diameter needs to be

$$B = \frac{f_c H(\theta)}{\rho_b g} \quad (10.13)$$

The next stage is to identify the unconfined yield stress for a powder inside a hopper, and to know more about the functional relation $H(\theta)$.

10.4 The powder flow function

We can represent the normal (σ) and shear stresses (τ) on a plane by an equation that describes a circle, this is the *Mohr's circle*. Adopting a coordinate system where the normal stress is plotted against the shear, Figure 10.10, the centre of the circle (C_c) is

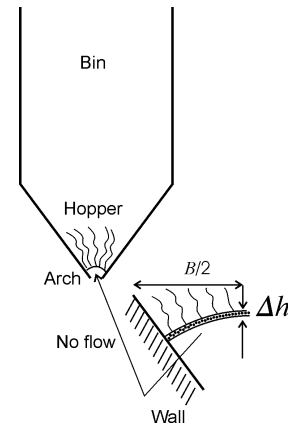


Fig. 10.9 Stable arch formed above the hopper outlet

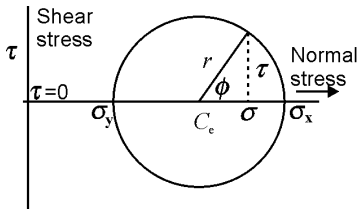


Fig. 10.10 Mohr's circle representing shear stress and normal stress on a plane by a circle

$C_e = \sigma_y + r$ and the radius (r) of the circle is

$$r = \frac{1}{2}(\sigma_x - \sigma_y) \tag{10.14}$$

Thus, by inspection and substitution the centre is also

$$C_e = \frac{1}{2}(\sigma_x + \sigma_y) \tag{10.15}$$

By Pythagoras' theorem for triangles

$$\tau^2 + (\sigma - C_e)^2 = \left[\frac{1}{2}(\sigma_x - \sigma_y) \right]^2 \quad \text{thus, from equation (10.15)}$$

$$\tau^2 = - \left[\sigma - \frac{1}{2}(\sigma_x + \sigma_y) \right]^2 + \left[\frac{1}{2}(\sigma_x - \sigma_y) \right]^2$$

and

$$\tau^2 = \left[\frac{1}{2}(\sigma_x - \sigma_y) \right]^2 - \left[\sigma - \frac{1}{2}(\sigma_x + \sigma_y) \right]^2 \tag{10.16}$$

i.e. in this coordinate system, equation (10.16) provides an equation to represent the shear and normal stresses, which is the equation of a circle where the centre is given by equation (10.15) and the radius by (10.14). The question now becomes: can the normal and shear stresses on a plane be represented by the above equation?

To answer this question the *principal planes* are considered, as illustrated in Figure 10.11. A plane of stress is resolved into two principal planes: where the shear (τ) and normal (σ) stresses of one plane are represented by two planes with *zero shear* acting. The resulting values are known as the maximum and minimum principal stresses, with an angle of 90° between the principal planes.

Now, these are planes of say length l and width m , and force is the product of stress and area (stress is similar to pressure). A force balance gives:

horizontally

$$lm \sin \theta \sigma_x + lm \cos \theta \tau = lm \sin \theta \sigma$$

$$\therefore \sigma_x + \frac{\tau}{\tan \theta} = \sigma \tag{10.17}$$

and vertically

$$lm \cos \theta \sigma_y = lm \cos \theta \sigma + lm \sin \theta \tau$$

$$\therefore \sigma_y = \sigma + \tau \tan \theta \tag{10.18}$$

Rearranging for $\tan \theta$ and combining these equations gives

$$\tau^2 = (\sigma - \sigma_x)(\sigma_y - \sigma) = \sigma \sigma_y - \sigma^2 - \sigma_x \sigma_y + \sigma \sigma_x$$

hence

$$\tau^2 = - \left[\sigma^2 - (\sigma_x + \sigma_y) \sigma \right] - \sigma_x \sigma_y = - \left[\sigma - \frac{1}{2}(\sigma_x + \sigma_y) \right]^2 - \frac{4}{4} \sigma_x \sigma_y + \frac{1}{4}(\sigma_x + \sigma_y)^2$$

and

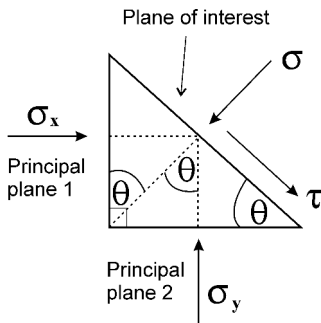


Fig. 10.11 Plane of interest resolved into two principal planes at right angles to each other - on the principal planes no shear acts.

$$\tau^2 = -\left[\sigma - \frac{1}{2}(\sigma_x + \sigma_y)\right]^2 + \frac{1}{4}(\sigma_y^2 - 2\sigma_y\sigma_x + \sigma_x^2)$$

Thus,

$$\tau^2 = \left[\frac{1}{2}(\sigma_x - \sigma_y)\right]^2 - \left[\sigma - \frac{1}{2}(\sigma_x + \sigma_y)\right]^2 \quad (10.19)$$

i.e. the equation of a circle in σ and τ coordinates, see equation (10.16) above. So, the principal planes illustrated above can be represented on a Mohr's circle. Note that the minor principal plane occurs where the normal stress axis (σ) is cut at the lower end of the circle ($\tau=0$) and the major principal plane is at the top end of the circle. We call these σ_y and σ_x respectively - see the Mohr's Circle diagram.

The angles between planes and in the Mohr's Circle are related, as can be seen from the vertical and horizontal force balances on the principal planes (rearranged for $\tan \theta$)

$$\tan \theta \tan \theta = \tan^2 \theta = \frac{\tau}{\sigma - \sigma_x} \frac{\sigma_y - \sigma}{\tau} = \frac{\sigma_y - \sigma}{\sigma - \sigma_x}$$

and using the general result

$$\tan 2\theta = \frac{2 \tan \theta}{1 - \tan^2 \theta}$$

So,

$$\tan 2\theta = \frac{2\tau}{\sigma - \sigma_x} \bigg/ \frac{1 - \frac{\sigma_y - \sigma}{\sigma - \sigma_x}}{\sigma - \sigma_x}$$

Hence,

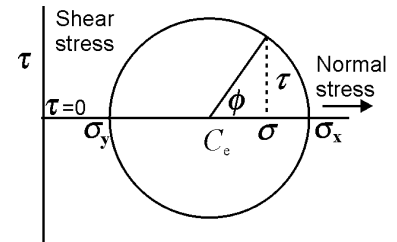
$$\tan 2\theta = \frac{2\tau}{2\sigma - \sigma_x - \sigma_y} = \frac{\tau}{\sigma - \frac{1}{2}(\sigma_x + \sigma_y)} \quad (10.20)$$

Comparing equations (10.20) and Figure 10.12, shows that

$$2\theta = \phi \quad (10.21)$$

i.e. the principal plane angle is half that given by the Mohr's circle.

We have now seen how it is possible to consider an arbitrary plane inside a powder compact, with both normal and shear stresses acting on it, and resolve it into two principal planes. A Mohr's circle represents shear stress (on the y axis) and normal stress (on the x axis). Hence, we can draw the shear condition of this arbitrary plane on these axes and obtain the equivalent minimum and maximum principal plane values. This is of interest if we know the stress condition that will cause the powder compact to break, or fracture. It is argued that the stress of interest is the maximum principal stress (σ_x): this represents the maximum stress consolidating the powder, i.e. giving it strength. Also of interest, for the purpose of breaking the powder compact, is the *unconfined yield stress* - again a maximum principal plane stress. The latter is obtained from the Mohr's circle



$$\tan \phi = \frac{\tau}{\sigma - C_e}$$

or

$$\tan \phi = \frac{\tau}{\sigma - \frac{1}{2}(\sigma_x + \sigma_y)}$$

Fig. 10.12 Mohr's circle with angle by inspection

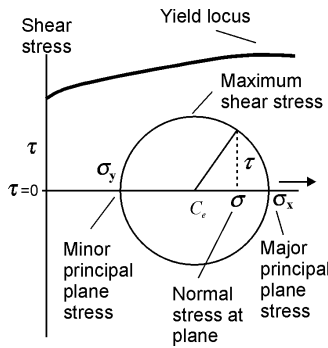


Fig. 10.13 Mohr's circle with yield locus - when a circle touches the yield locus failure occurs

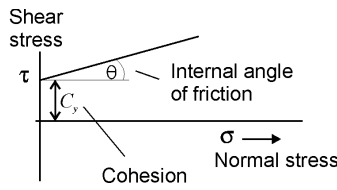


Fig. 10.14 Cohesion and friction in a Coulomb solid

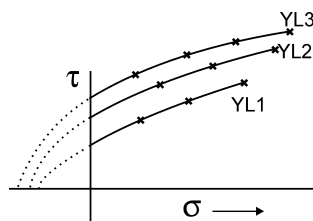


Fig. 10.15 Yield loci for powder compact

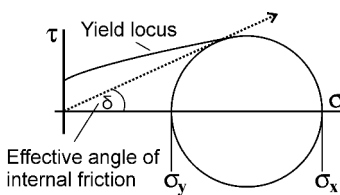


Fig. 10.16 Effective angle of internal friction

that must also go through the origin. Before we see this in practice we should consider the Mohr's circle a bit further.

If we increase the normal, or shear stress, on a powder the Mohr's circle representing it will become bigger, see Figure 10.13. If we know where the yield locus lies, then the circle can only become bigger until it touches the yield locus. Note that if we treat powder compacts as *Coulomb solids* the yield locus cuts the shear stress axis (i.e. does not go through the origin) and usually has a small positive gradient. For a given powder compact the maximum principal stress can be obtained by drawing a Mohr circle that is *tangential* to the yield locus at the upper end. The corresponding unconfined yield stress comes from drawing a Mohr circle again tangential to the yield locus, but with the minor principal plane stress going through the origin (i.e. unconfined with zero stress acting).

However, the Coulomb solid formed by the powder compact will have properties that depend upon how it has been treated. The greater the original consolidating load, the larger will be the yield locus. Hence, a series of yield loci will exist for a given powder, dependent upon the consolidation conditions used to form the compact. This series of yield loci can be used to provide a relation between the strength of the powder to resist breakage and the consolidating conditions used to form the compact; this is the material, or powder, flow function.

In a Coulomb solid there is a limit to the range of stresses that will cause no permanent deformation. A stress equal to the limit causes plastic flow, see Figure 10.14, where C_y is similar to a yield stress and is called the *cohesion*

$$\tau = \sigma \tan \theta + C_y \quad (10.22)$$

Equation (10.22) provides the shear stress needed to cause failure of the specimen at a given normal force. A free flowing powder will have no cohesion, resulting in a line through the origin ($C_y=0$). For cohesive powders, a *shear cell* can be used to determine a yield locus where the powder is first consolidated to a given bulk density and state, then sheared under different values of consolidating load or normal stress. The tests can be repeated to provide several yield loci for the same powder, but under conditions of different initial consolidation, see Figure 10.15.

The top point on each locus was obtained from a powder by applying a fixed consolidating load *before* and *during* the shear test. The same load was initially applied for all the other tests used, but lower values were used *during* the test; the powder retains the properties of the material formed during the pre-shear consolidation process. The highest pre-shear consolidation load was used for YL3, and YL1 had the lowest. The powder porosity should decrease with increasing consolidating load so YL3 represents the strongest and least porous powder compact.

The *effective angle of internal friction* is given by the angle of a line going through the origin that is tangential to the Mohr's circle drawn at the end of the yield locus, see Figure 10.16, and compare with Figure 10.14.

Consideration of the Mohr's circle, provides two key elements that are used in the characterisation of powders and hopper design: the *unconfined yield stress* (f_c) and the *maximum principal stress* (σ_x). The unconfined yield stress is the maximum stress on a powder plane where the other principal plane is under conditions of zero shear and zero consolidation. This is the condition at the open side of a stable arch, - see Figure 10.9. So, in order to break a stable arch - or to stop one forming, we need to ensure that conditions within the hopper are such that the state of stress is greater than the unconfined yield stress, as given by the Mohr's circle going through the origin and tangential to the yield locus. The physical state of the powder is given by the consolidation conditions; treating the powder as a Coulomb solid the powder strength will be greater when the consolidation forming the compact is greater. The powder has been formed by the conditions of shear stress and consolidation given by τ_a and σ_a respectively. However, under the Mohr's circle development, we may represent this state of stress as a single (maximum) principal plane stress σ_x . Perhaps the best way of considering these parameters is to think of a maximum consolidating stress (σ_x) that will give rise to a single value of the unconfined yield stress (f_c). The greater the consolidation then the stronger the powder: hence the larger the value of f_c and the hopper will have to be designed to provide a greater arch breaking condition: e.g. steeper angle from the horizontal or larger opening. These terms are illustrated in Figure 10.17.

This relation between the unconfined yield stress and the maximum consolidation stress is often a single repeatable function that characterises how the powder compact behaves; it is known as the *Powder Flow Function* (PFF), or *Material Flow Function* (MFF). For cohesive powders, it is a more useful and reliable form of powder characterisation than angle of repose, etc.

The PFF is obtained by the following methodology. A single yield locus is used to provide the Mohr's circle that can be fitted to the stress condition at the end of that locus: i.e. a circle is drawn through the top point of the locus such that it is tangential to the locus. The maximum consolidating principal stress is read off where the Mohr's circle cuts the normal stress axis. The unconfined yield stress comes from another Mohr's circle plotted near the origin: the minimum normal stress has to be at the origin and the circle must again be tangential to the yield locus, see Figure 10.17. The unconfined yield stress is read off where this Mohr's circle cuts the normal stress axis. The two values are plotted as a single data point on the illustrated PFF (or MFF) graph. This procedure provides one data point for the PFF, so other yield loci must be obtained (under different consolidation conditions) to provide sufficient data to draw the full

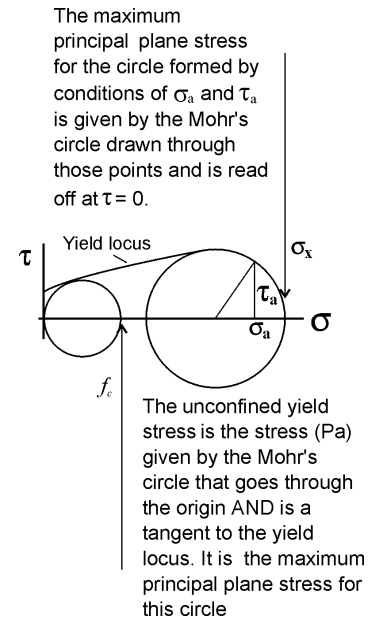


Fig. 10.17 Construction for the required data for the PFF

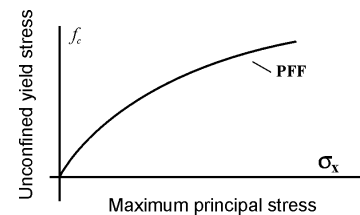


Fig. 10.18 The Powder Flow Function

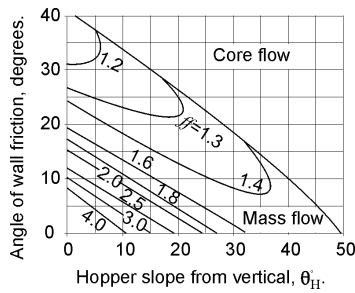


Fig. 10.19 Jenike design chart for a powder with an effective angle of internal friction of 50°

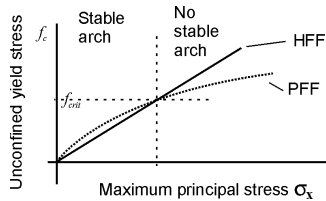


Fig. 10.20 Test for flow by comparing the PFF and the HFF

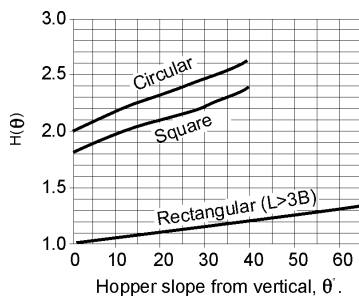


Fig. 10.21 $H(\theta)$ for types of hopper opening where L is one rectangular dimension and B the other: if $L < 3B$ use the square curve

curve. The origin on the unconfined yield stress and maximum consolidation stress figure provides an additional data point. An illustrative PFF is shown in Figure 10.18.

For the powder we now know: the PFF and the effective angle of internal friction, from Figure 10.16, which tells us something about how stress will be transmitted within the powder. Thus, we have characterised our powder and must consider the state of stress in the powder caused by the hopper design and see whether it will be sufficient to overcome the formation of a stable arch.

10.5 The hopper flow factor and hopper design

To determine the *Hopper Flow Factor* (HFF) the following procedure is used: the appropriate *Jenike design chart* is identified using the effective angle of internal friction. The angle of wall friction is obtained from tests described later and the hopper slope from the vertical is either measured, for an existing hopper, or selected for a new design. The value selected is based on the knowledge that the design chart, an example is illustrated in Figure 10.19, is split into two regions. The bottom left region is for a mass flow hopper and the top right will result in a core flow hopper. Thus, a value of the hopper slope from the vertical that rests on the dividing line between these regions is bordering on a mass flow design. For the sake of safety, assuming that a mass flow design is required, it is usual to come 3 degrees back towards the vertical and into the mass flow regime from this line. On the design chart, the hopper ratio between compacting stress and applied shear stress (ff) is estimated, and the HFF is plotted on the same graph as the PFF, as a line with gradient of $1/ff$, Figure 10.20.

To test for a stable arch in the hopper the following logic is applied. Where the PFF lies *above* the HFF the powder has greater strength to resist shear and collapse than the hopper/powder system can provide. A stable arch is, therefore, possible. When the HFF is above the PFF the system has sufficient stress to break an arch and reliable flow should exist. The point at which the PFF and MFF meet gives the *critical unconfined yield stress* ($f_{c-critical}$) and this can be used to determine the minimum hopper opening, from equation (10.13)

$$B = \frac{f_{c-critical} H(\theta)}{\rho_b g} \tag{10.23}$$

where $H(\theta)$ is a constant dependent upon the geometry of the hopper opening. The factor $H(\theta)$ arose in the derivation of the stable arch where the arch was assumed to act over a linear distance L , which acts up to the centre of the hopper. The arch forms above the opening but the linear dimension measured, or deduced, is the hopper opening itself. This is not the same as L , or even $2L$, but bears some relation to it. Jenike provided another chart, Figure 10.21, for this relation, dependent upon the opening geometry and the hopper slope from the vertical.

10.6 Measurement techniques and conditions

The simplest way to determine the unconfined yield stress is from a Uniaxial Compression test, see Figure 10.22. Firstly, the powder is compacted whilst constrained by the application of a normal consolidating load. The constraints are then removed and another compressive load applied. The value of this load at the point of failure is the unconfined yield stress; i.e. no side-walls and no shear stress; solely a consolidating stress applicable at the point of failure. It is fairly easy to relate this state of affairs to that of breaking an arch inside a hopper. However, the uniaxial compression test is not a reliable method. The most common method employed is the Jenike shear cell.

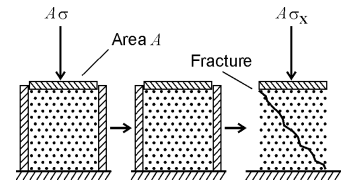


Fig. 10.22 Uniaxial compression test

During the Jenike test, Figure 10.23, two rings are employed (upper and lower). The powder fills the rings and has a consolidating load applied. This load is removed and a lower load applied, together with a shear stress via the bracket on the side of the top ring. When the shear stress is sufficient the top ring will slide over the bottom, and the powder has sheared. This gives one value for shear and consolidating stress, which may be plotted on a yield locus. A measurement of wall friction can be achieved simply using the top ring from the Jenike shear cell: a given normal force is applied and the shear force required to slide the ring over the solid surface can be measured. A series of experiments at different normal forces gives rise to a graph from which the angle of friction can be deduced.

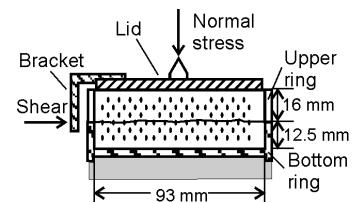


Fig 10.23 Jenike shear cell

Using a load cell connected to a chart recorder the trace (i.e. shear load) should increase steadily until the powder yields. This will be the proper consolidation curve, or plot, illustrated in Figure 10.24. However, if the powder only forms a loose aggregate the trace will follow the under consolidated curve. Conversely, if the powder is so tightly consolidated that dilatancy needs to be overcome (i.e. the powder must expand before it can shear) then the over consolidated curve will be followed. Only the test result from the proper consolidation should be used.

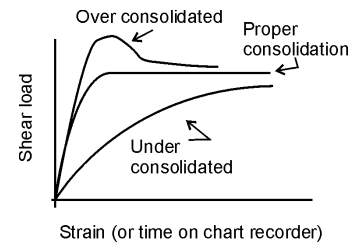


Fig. 10.24 Test for correct consolidation

An alternative to the Jenike cell is the Ring Shear Tester, Figure 10.25. Again a normal force is applied together with a shear or rotational stress, see Powder Handling and Processing, Vol 8, No. 3, 1996, pp 221 - 226, or <http://members.aol.SchulzeDie/grdle1.html> for further details.

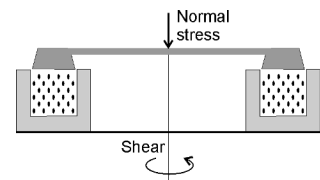


Fig. 10.25 Ring shear cell

If the powder is left for some length in time, then the compact usually becomes stronger due to *time consolidation*. Hence, a new yield loci, and powder flow function (usually stronger), will be formed. The strength of a powder is also greatly influenced by the prevailing *humidity*. Hence, it is important to conduct the tests under controlled humidity conditions that will be similar to that used for powder storage.

A triaxial test cell, consisting of a rubber sleeve around a cylinder of powder with side stress applied together with compressing stress at the ends, can be used to investigate compact failure. The

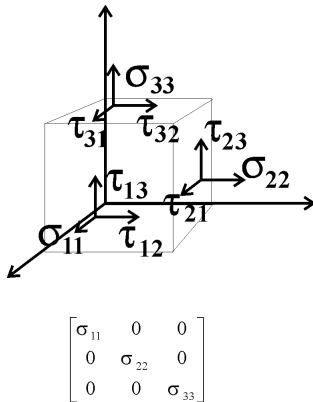


Fig. 10.26 Three dimensional consideration of stresses with principal plane matrix below

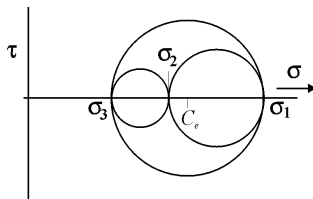


Fig. 10.27 Three dimensional representation on Mohr's circles

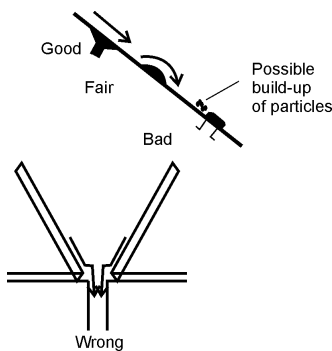


Fig. 10.28 Hopper fastener and discharge arrangements to avoid arch formation

continuum approach in three dimensions is illustrated in Figure 10.26, showing an element, or cube, of material with the corresponding stress tensor

$$\begin{bmatrix} \sigma_{11} & \tau_{12} & \tau_{13} \\ \tau_{21} & \sigma_{22} & \tau_{23} \\ \tau_{31} & \tau_{32} & \sigma_{33} \end{bmatrix} \quad (10.24)$$

However, consideration of only three mutually perpendicular principal planes (no shear forces acting) results in the simpler matrix shown in Figure 10.26, which can be drawn as a tetrahedron, or pyramid, with three principal planes (x,y,z) that represent the resolved forces from a plane joining the three principal planes. The corresponding three dimensional Mohr's circle, represented on two dimensional paper, can be drawn as three circles and is shown in Figure 10.27.

In order to maintain stable discharge from a hopper many *bin inserts* have been marketed. The formation of a stable arch may be disrupted by surfaces placed close to where an arch is most likely to form. See Lyn Bates, *The Chemical Engineer*, 14 November 1996 and numerous articles at: www.powderandbulk.com/. Consideration of the fastener arrangement, and discharge system, within the hopper is also important. Some examples of these are shown in Figure 10.28.

10.7 Summary

The hopper design procedure is summarised as follows: when considering a powder for the first time a series of yield loci can be obtained by laboratory measurements and the Powder Flow Function (PFF) deduced. The effective internal angle of friction is also obtained and the appropriate Jenike design chart identified. Tests also give the wall friction. For mass flow conditions (no arch and uniform flow), the operating region should be in the bottom left section of the Jenike design chart. For the sake of safety, it is usual to come three degrees back into the mass flow regime, i.e. reduce the hopper angle *from* the vertical axis. This is, therefore, the hopper half angle. The hopper flow factor is also deduced from this chart. A plot of the hopper flow factor and PFF can be used to deduce the critical unconfined yield stress and, therefore, the minimum hopper opening from equation (10.23). Hence, the hopper is now specified in terms of angle and opening diameter; storage capacity per silo can be deduced from the geometry and the maximum discharge rate can be estimated from the empirical equation (10.2), but this neglects coherency and should only be used as a rough estimate.

The powder flow function is useful for hopper design, but is also a property of the powder and can be used as a characterisation technique in itself. For example, it may be used to correlate some behaviour within a process, or from a product, with the PFF.

However, changes with the PFF dependent upon humidity and time should be considered.

Apart from powder storage in silos, other common powder containers include an *Intermediate Bulk Container* (IBC), which is a large sack that can hold over 1 tonne of powder. For transportation of amounts in excess of IBC values trucks and wagons are needed.

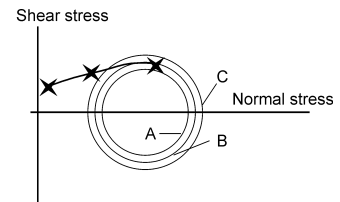
See:
www.jenike.com
 for more information on
 hopper design

10.8 Problems

Explain and answer the following terms:

- | | | |
|----------------------------|-------------------------|------------------|
| Dilatancy | Segregation | Shear stress |
| Critical Porosity | Normal stress | Principal stress |
| angle of internal friction | angle of wall friction | |
| effective yield locus | powder flow function | |
| hopper flow factor | unconfined yield stress | |

- Mohr circle (why is the centre always on the $\tau=0$ line)?
- Given any value of τ and σ on a Mohr circle, at what angle to a principal plane will failure occur?
- Give physical meaning to the points at the opposite end on a Mohr's circle lying on the axis $\tau=0$.
- How does increasing the state of stress influence the Mohr circle?
- What is the yield locus and why is it a locus?
- Sketch the yield locus of a free flowing powder and a cohesive powder - is the latter a meaningful question?
- Why is the maximum consolidation stress important?
- Please explain the condition required for a stable arch.
- A, B and C are badly drawn Mohr circles, together with three data points from a yield locus. Explain what is happening as the state of stress goes from A, through B and on to C. Do they all really exist?



10. A Jenike shear test on a powder resulted in the following data:

	Normal stress Pa	Shear stress Pa	Normal stress Pa	Shear stress Pa	Normal stress Pa	Shear stress Pa
Maximum normal load	2200	1340	1600	1000	1200	740
At subsequent loads	1600	1250	1000	920	900	740
	1000	1100	700	840	600	640
	400	900	400	700	400	560

Derive the powder flow function for the powder. If the material is hygroscopic, outline a series of tests to check on the importance of changes in humidity on the hopper design.

11. Draw a diagram representing the variation of solids stress inside a silo, and explain its shape. Contrast the solids stress with the variation of hydrostatic liquid pressure.

The following results were obtained using a Jenike shear cell with time consolidation of 0, 7 and 14 days. Obtain the theoretical minimum opening for a cylindrical silo of hopper half angle 30° , $H(\theta)$ of 2.2 and angle of wall friction of 15° . Use a powder bulk density of 1800 kg m^{-3} .

0 Days		7 Days		14 Days	
$f_c \text{ kN m}^{-2}$	$\sigma_x \text{ kN m}^{-2}$	$f_c \text{ kN m}^{-2}$	$\sigma_x \text{ kN m}^{-2}$	$f_c \text{ kN m}^{-2}$	$\sigma_x \text{ kN m}^{-2}$
2.6	3.0	5.5	7.0	9.0	10.0
3.1	5.5	5.7	9.0	9.2	12.0
3.4	8.0	5.9	12.0	9.3	14.0

The actual hopper opening is 1 m in diameter; determine the time that the powder can be left in the hopper without arching. If this time is too short what steps can be used to ensure that the material still flows reliably?

12. Intermittent flow is experienced from a cylindrical silo with a conical hopper that is several years old. The design criteria have been checked by remeasuring the powder properties and wall friction. The powder properties were found to be unchanged but it was discovered that the hopper wall had become badly scored. Using the following data and Figures 10.19 and 10.21 determine what minimum diameter opening is now required. What solution would you offer to ensure that the problem will not recur?

Powder characteristics:

Bulk density: 1800 kg m^{-3}

Unconfined yield stress kPa	8.5	5.8	3.0
Maximum consolidation stress kPa	16.0	10.0	3.5

Wall friction results

In 1998	Normal stress kPa	8.00	4.00	2.00
In 1998	Shear stress kPa	1.41	0.71	0.35
In 2002	Normal stress kPa	8.00	4.00	2.00
In 2002	Shear stress kPa	3.23	1.62	0.81

Hopper half angle is 15° .